IEEE Access
Multidisciplinary | Rapid Review | Open Access Journal

Received January 7, 2021, accepted January 19, 2021, date of publication January 25, 2021, date of current version February 3, 2021.

Digital Object Identifier 10.1109/ACCESS.2021.3054434

Tunable Frequency Selective Surface Based on a Sliding 3D-Printed Inserted Dielectric

SHIHAO QIU, (Graduate Student Member, IEEE), QINGXIN GUO, (Senior Member, IEEE), AND ZENGRUI LI, (Member, IEEE)

State Key Laboratory of Media Convergence and Communication, Communication University of China, Beijing 100024, China

Corresponding authors: Shihao Qiu (qiush79@126.com) and Zengrui Li (zrli@cuc.edu.cn)

This work was supported in part by the National Natural Science Foundation of China (NSFC) under Grant 62071436, Grant 62071435, and Grant 61671415; in part by the Fundamental Research Fund for the Central Universities under Grant CUC19ZD001; and in part by the Key Laboratory of All Optical Network and Advanced Telecommunication Network, Ministry of Education, Beijing Jiaotong University under Grant ZG19002.

ABSTRACT A novel mechanically tunable frequency selective surface (FSS) based on a sliding 3D-printed inserted dielectric is presented in this paper. This paper first introduces the working mechanism of the tunable FSS, which indicates that the variable capacitance is the key to tunability. Based on this, we design an all-metal bandpass FSS with a certain thickness and a matching cross-shaped inserted dielectric. By changing the insertion depth of the dielectric, the resonance frequency can be adjusted. To optimize the performance, an improved structure based on a hollow support and a tripole slot is proposed. A tunable range from 3.24 to 5.52 GHz (53%) and good angular stability is obtained in the simulation. To verify this idea, we fabricate a cross slot prototype by 3D printing and mechanical engraving. Measured results show that this prototype has a continuous tunable range of 3.61 to 5.89 GHz (34.4%).

INDEX TERMS Frequency selective surface (FSS), tunable, 3D printing, dielectric.

I. INTRODUCTION

A frequency selective surface (FSS), as a kind of spatial filter, has been widely used in the radome, antenna and EM absorber fields. A traditional FSS is a passive structure, which is usually composed of periodic metallic slots or patches printed on a substrate. These FSSs generally exhibit bandpass or bandstop characteristics. With the increasing complexity of microwave technology and electromagnetic environment, the performance demand for FSSs is growing. FSSs with different properties, such as high selectivity, multi-polarization, tunability and angular stability, are the trend of future development. Among them, a tunable FSS has been of wide concern and extensively studied in the past decades.

At present, tunable FSSs can be implemented in various ways, which can be roughly divided into the following categories:

(1) Tunable FSS loaded with active components [1]–[8]. This is a well-known implementation of a tunable FSS. The active components could be varactor diodes, PIN diodes, Schottky diodes, etc. By adjusting the applied voltage of the active device, the resonance frequency of the FSS can be changed. This method can ensure a compact structure and a wide tunable range. However, the disadvantage is that active components need a feed network and an external power supply. Adding a bias network and isolating elements will also affect the original frequency response of the FSS, which may result in poor selectivity or a large insertion loss. In addition, the complex structure and too many active components also increase the manufacturing cost and restrict the practicability.

(2) Tunable FSS based on an active dielectric. This method is realized by using materials with adjustable electrical properties, such as the liquid crystal mentioned in [9]. By applying a changing voltage to the liquid crystal, the permittivity can be adjusted and tunability is achieved. Similar published designs include those using barium strontium titanate (BST) [10], [11], graphene [12], etc.

(3) Mechanically tunable FSS. This kind of tunable FSS is generally novel and interesting and has been achieved by, for example, changing a spring height via pressure to adjust the resonance frequency [13], or using pressure-driven fluidic control of mercury volumes [14]. Other examples included the use of a liquid metal [15], a rotatable square [16]

The associate editor coordinating the review of this manuscript and approving it for publication was Yuh-Shyan Hwang.

and an origami structure [17]. Some designs also apply micro-electro-mechanical systems (MEMS): [18] placed MEMS metallic bridges over slots to achieve tenability, whereas [19] used a MEMS rotating-dipole array to alter the resonance frequency.

The new tunable FSS proposed in this paper is inspired by the control rods of a nuclear reactor, which control the rate of chain reaction by changing the depth of insertion. A similar structure could be used in FSSs. The mechanism is based on changing the insertion depth of a dielectric in the slot of a bandpass 3D-FSS to control the equivalent capacitance and finally tune the resonance frequency.

After the introduction to tunable FSS development, the following content is divided into three parts. Section II explains the design principles of the proposed tunable FSS and shows the simulated results. We fabricated a prototype to verify this idea and show the measured results and photographs in Section III. The last Section IV presents the conclusion of this work.

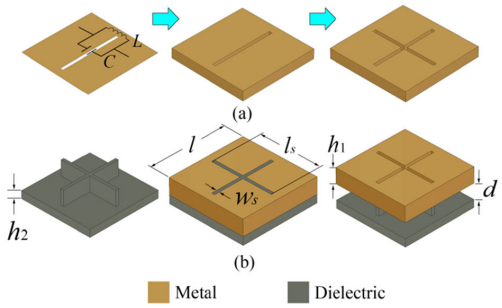

FIGURE 1. Design process of the tunable FSS. (a) Traditional planar bandpass FSS and 3D-FSS. (b) Inserted dielectric and tunable FSS. (l = 30 mm, l_s = 26 mm, w_s = 1.5 mm, h_1 = 8 mm and h_2 = 4 mm; d is the retraction depth with a tuning range of 0 to h_1.).

II. DESIGN PRINCIPLES AND SIMULATION

A typical bandpass FSS is a periodic slot structure and can be described by equivalent circuit theory [20], as shown in Fig. 1(a). The slot is equivalent to a capacitor, and the narrow metallic strip is equivalent to an inductor. They form a parallel LC resonator. Therefore, the resonance frequency f_s of the bandpass FSS can be expressed as:

$$f_s = \frac{1}{2\pi\sqrt{LC}}. \tag{1}$$

Different from the traditional planar structure, the tunable FSS proposed in this paper is based on a bandpass all-metal 3D-FSS, as shown in Fig. 1(a). The slot with a certain depth can be equivalent to a parallel-plate capacitor, and its value is roughly calculated by (2).

$$C = \frac{\varepsilon_0\varepsilon_r S}{w_s} = 8.85 \times \frac{\varepsilon_r l_s h_1}{w_s}(\text{pF}). \tag{2}$$

According to (1), the tunability of f_s can be achieved by changing the value of C. To realize this purpose, a cross-shaped dielectric with a support plate under it is designed, as shown in Fig. 1(b). The dimension of the cross-shaped

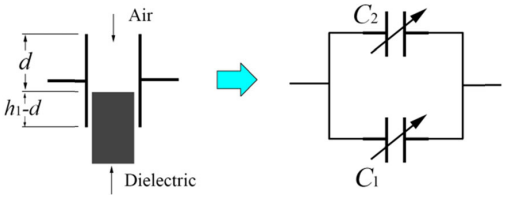

FIGURE 2. Working mechanism of the proposed tunable FSS.

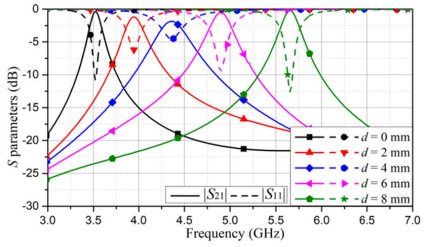

FIGURE 3. Simulated S parameters results under normal incidence.

dielectric is just similar to the slot in the metal. Hence, it can fill the slot if it is completely inserted. The cross-shaped dielectric, together with the support plate, is manufactured by 3D printing.

Fig. 2 explains the operation mechanism of the resonance frequency variation. When the inserted dielectric is slid into the slot, the composition in the slot will consist of air and the dielectric, and tuning the retraction depth d will change the ratio of the two. In other words, this slot can be equivalent to two parallel variable capacitors. Without regard to the effect of edge capacitance, the total capacitance can be roughly expressed as:

$$\begin{aligned} C &= C_1 + C_2 \\ &= 8.85 \times \frac{\varepsilon_r l_s (h_1 - d)}{w_s} + 8.85 \times \frac{l_s d}{w_s}(\text{pF})(0 \le d \le h_1). \end{aligned} \tag{3}$$

According to (3), the tunability appears to be mainly affected by the relative permittivity of the dielectric. In this model, the inserted dielectric is taken as a polymer resin with $\varepsilon_r = 3.8$, which is a widely used material for 3D printing. Notably, in the following simulations, we assume that the dielectric is lossless and ε_r does not vary with frequency. In fact, most 3D-printed materials do not have good frequency stability. A loss tangent and a slight decrease in the relative permittivity are inevitable.

The simulated S parameters under normal incidence are calculated and shown in Fig. 3. As the retraction depth d of the dielectric changes from 0 to 8 mm, the resonance frequency rises from 3.53 to 5.58 GHz (45.0%). In addition, the minimum and maximum insertion losses are 0.13 dB and 1.87 dB, respectively. We consider that the insertion loss may be mainly caused by the reflection of the support plate.

Furthermore, the simulated $|S_{21}|$ results under oblique incidence are shown in Fig. 4(a). As the incident angle increases, several obvious grating lobes appear at high frequency, especially when the dielectric is completely retracted

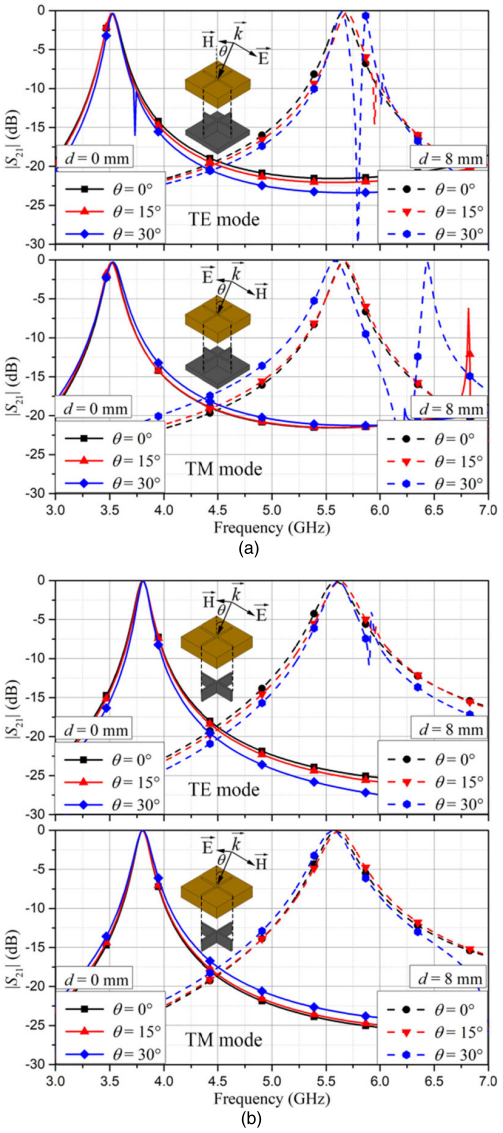

FIGURE 4. Simulated $|S_{21}|$ results under oblique incidence. (a) With the support plate. (b) Without the support plate.

($d = 8$ mm, $\theta = 30°$). The results show that this model appears to have poor angular stability. We consider that the support plate degrades the oblique incidence performance. For comparative analysis, the simulated $|S_{21}|$ results without the support plate are also shown in Fig. 4(b). The angular stability is significantly improved. Therefore, using a hollow structure to support the inserted dielectric is a better choice.

To achieve optimal performance, we present several investigations with different parameters. Fig. 5(a) and Fig. 5(b) shows the simulated $|S_{21}|$ with changing slot width w_s and slot depths h_1, respectively. From these two figures, as the slot width decreases or the depth increases, the passband selectivity improves, but the resonance frequency and tunable range do not change. In other words, a large thickness does not appear to be strictly necessary for this tunable FSS.

Additionally, the simulated results for different relative permittivities are shown in Fig. 5(c). The increase in ε_r causes

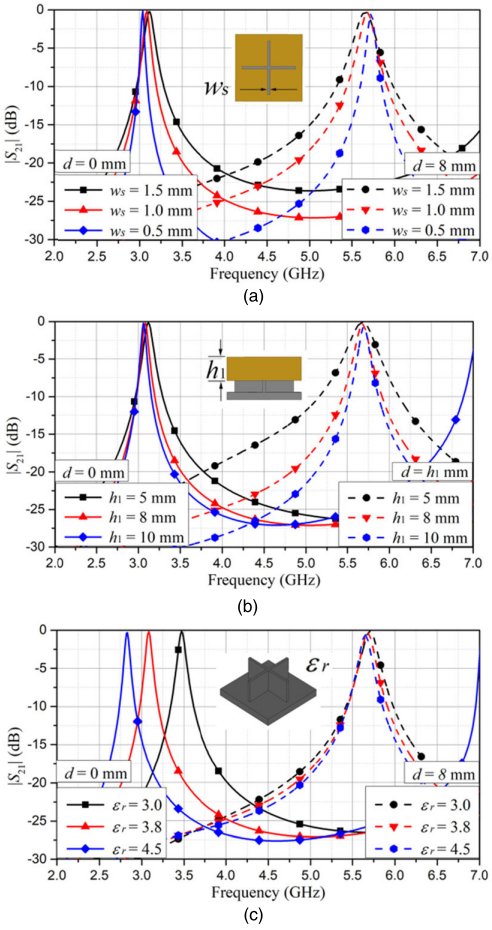

FIGURE 5. Simulated $|S_{21}|$ results with several changing parameters. (a) Slot width w_s. (b) Slot depth h_1. (c) Relative permittivity ε_r.

the minimum frequency to decrease from 3.47 to 2.83 GHz, but the insertion loss rises from 0.16 to 0.32 dB. These results indicate that the larger ε_r is, the lower the minimum tunable frequency, but the maximum tunable frequency remains unchanged. In conclusion, the tunable range clearly depends on the relative permittivity of the dielectric, but a large relative permittivity may cause more reflection.

Based on the optimization, we propose an improved structure, as shown in Fig. 6. To obtain better angular stability, the cross slots are changed to tripole slots. The slot depth h_1 and width w_s of the 3D-FSS are reduced to 4 mm and 1 mm, respectively. The support structure is designed as a hexagonal grid. By adjusting the screws around it, the insertion depth of the entire dielectric grid can be conveniently changed.

The simulated S parameters of the improved tunable FSS are shown in Fig. 7. A tunable range from 3.24 to 5.52 GHz (53%) is obtained. The insertion loss ranges from 0.12 to 0.2 dB. The results show that the hollow support structure significantly reduces the insertion loss. The simulated $|S_{21}|$ results under oblique incidence are shown in Fig. 8. In TM mode, the structure has good angular stability when the incident angle is scanned from 0° to 45°. In TE mode, the grating lobes still exist at high frequency, but the grating

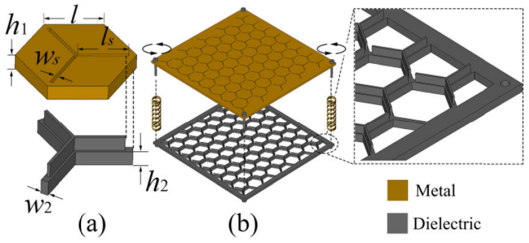

FIGURE 6. Improved structure based on a hollow support and a tripole slot. (a) Unit cell. (b) Overall structure. (l = 15 mm, l_s = 13 mm, w_s = 1 mm, w_2 = 2 mm, h_1 = 4 mm and h_2 = 4 mm.).

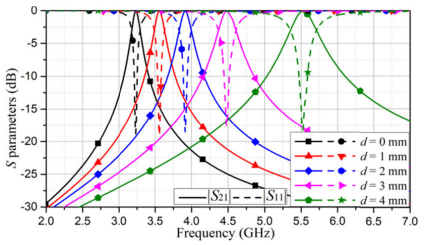

FIGURE 7. Simulated S parameters results of the tripole slot tunable FSS under normal incidence.

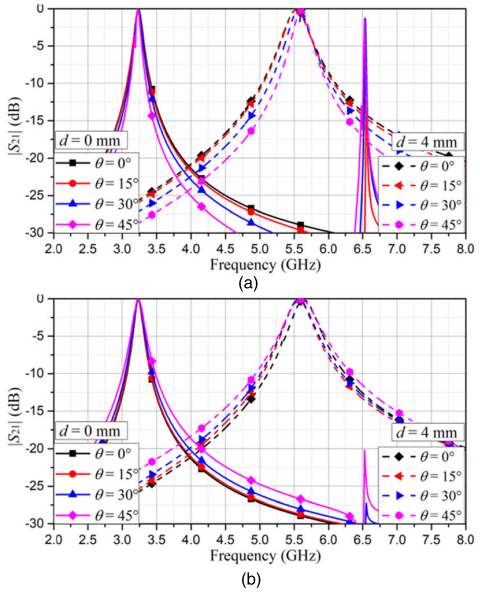

FIGURE 8. Simulated $|S_{21}|$ results of the tripole slot tunable FSS under oblique incidence. (a) TE mode. (b) TM mode.

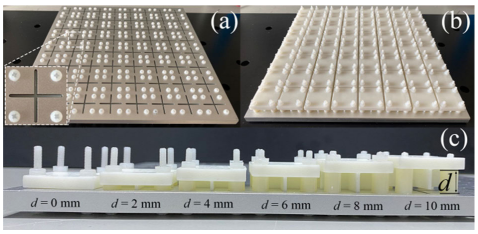

FIGURE 9. Photographs of the tunable FSS prototype. (a) Front side. (b) Back side and inserted dielectric. (c) Demonstration of different retraction depths d from 0 to 10 mm.

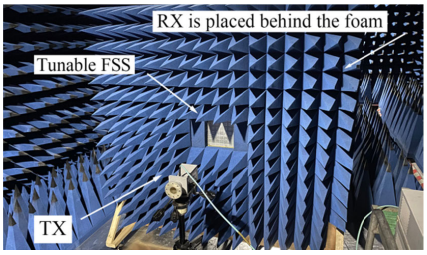

FIGURE 10. Photograph of the measurement system.

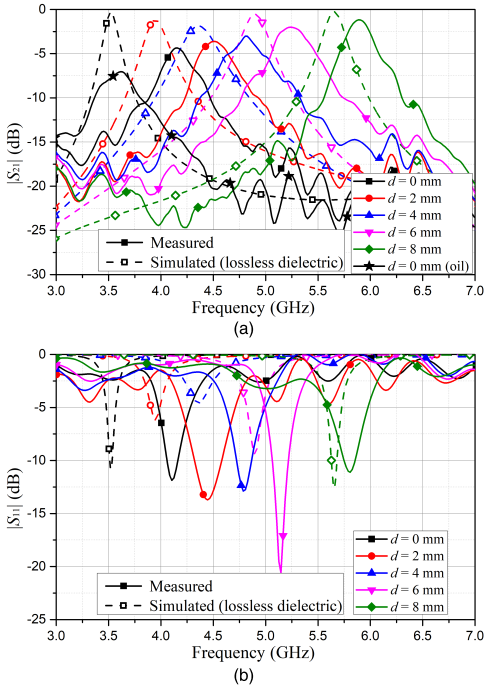

FIGURE 11. Comparison of measured and simulated S parameters of the tunable FSS prototype. (a) $|S_{21}|$. (b) $|S_{11}|$.

lobes near the passband have been eliminated. Compared with the simulated results shown in Fig. 4, the angular stability of the tunable FSS based on the hollow support and a tripole slot has been greatly improved. According to this example, the idea proposed in this paper appears to have good universality. Tunability of bandpass FSSs based on various shapes could be achieved through this method.

III. MEASUREMENT AND DISCUSSION

A prototype based on a cross slot with a 240 mm × 240 mm size (8 × 8 units) was fabricated to verify this idea, as shown in Fig. 9. The materials of the metal 3D-FSS and the inserted dielectric are aluminum and polymer resin (ε_r = 3.8), respectively. Plastic screws and studs of different sizes are used to adjust the retraction depth d. The dielectric could have been conveniently print in a whole piece, but the pieces were separately printed to ensure accurate operation of this prototype.

We measured the prototype in an anechoic chamber by using a transmitting antenna (TX), a receiving antenna (RX), and a VNA (Agilent E5071C), as shown in Fig. 10. The test sample is surrounded by absorbent foam to reduce the edge

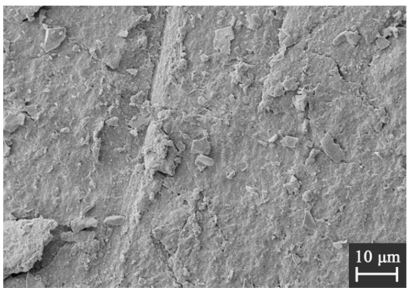

FIGURE 12. SEM photograph of the surface of the 3D-printed inserted dielectric made of polymer resin.

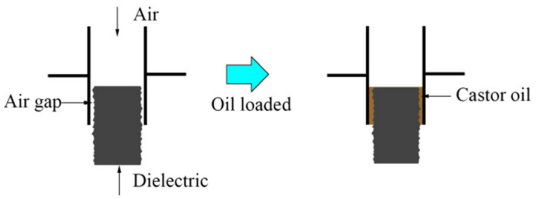

FIGURE 13. Filling of the air gaps with castor oil.

TABLE 1. Performance comparison.

Ref.	Configuration	Tunable range (GHz)	I.L.[1] (dB)	Thick-ness (λ_L[2])	Polariz-ation
[1]	3D-structure with varactor	1.4-2.75 (65%)	1-4.5	0.15	Single
[2]	Multilayer FSS with varactor	3.7-5.2 (34%)	3-6	0.1	Dual
[4]	Multilayer FSS with varactor	2.92-4.66 (46%)	1-4.5	0.12	Dual
[13]	Spring resonator	3.2-3.8 (17%)	< 1	0.28-0.38	Dual
[15]	Liquid metal	8-11.2 (33%)	< 1	N.A.	Single
[18]	MEMS bridge	8.5-10.3 (18%)	3.6-6.4	N.A.	Single
This work	Inserted dielectric (Sim. Fig. 6)	3.2-5.5 (53%)	< 1	0.08-0.13	Dual
	Inserted dielectric (Mea. Fig. 9)	4.16-5.89 (34%)	1.2-4.4	0.17-0.28	Dual

[1]I.L. = insertion loss.
[2]λ_L = the wavelength of the lowest frequency in the tunable range.
Since the loss tangent of the 3D-printed material is unavailable, the simulation in Fig. 6 used a lossless material.

diffraction effect. The measured and simulated S parameters under normal incidence are shown in Fig. 11. A range of resonance frequency from 4.16 to 5.89 GHz (34.4%) is obtained in the measurement. Compared with the simulated results shown in Fig. 3, the measured tunable range is significantly reduced. The main reason is that the machining tolerances in 3D printing make the cross-shaped dielectric unable to fill the slot completely. The scanning electron microscope (SEM) photograph of the dielectric surface shown in Fig. 12, reveals that the surface of the dielectric is uneven and grainy, which inevitably results from the operating mechanism of the 3D printer. Therefore, air gaps are sandwiched between the metal and the dielectric, reducing the tunable range of equivalent capacitors.

To mitigate the impact of the air gaps, we applied castor oil ($\varepsilon_r = 4.7$) on the surface of the dielectric to fill in the air gaps, as shown in Fig. 13. Castor oil is widely used in mechanical lubrication, and it is also commonly used as a capacitor electrolyte. The measured results with castor oil loaded are also shown in Fig. 11(a). From this result, the minimum frequency decreases from 4.16 to 3.61 GHz, which is close to the simulated value. This indicates that the reduced tunable range should be mainly caused by air gaps. However, the prototype with castor oil loaded is difficult to accurately adjust.

On the other hand, as the frequency increases, the insertion loss reduces from 4.35 to 1.17 dB. The main cause of the insertion loss in the measurement is the loss tangent of the 3D-printed material. Because the electric field in the inserted part of the dielectric is larger than that in the outside part, more energy is lost as the insertion depth increases. Therefore, the insertion loss increases as the frequency decreases.

Finally, the performance comparison of several published tunable FSS structures is shown in Table 1. Compared with other mechanical designs, our design has obvious advantages: wide tunable range, simple structure, and easy realization of dual polarization. Tunability of the traditional planar bandpass FSS can be easily achieved by changing it to a three-dimensional structure and inserting a matching shaped dielectric. Due to the working mechanism of this tunable FSS, the original shape and characteristics of the FSS can be well preserved.

However, some apparent shortcomings need to be improved:

(1) The 3D-printed dielectric in this paper has a large loss. Using more suitable materials could reduce the insertion loss.

(2) The 3D-FSS needs a certain thickness to achieve tunability. Notably, the thickness does not influence the operating wavelength or tunable range, so it could be appropriately reduced.

(3) Accurately adjusting the dielectric as a whole is difficult. The larger the area of the FSS is, the more difficult it is to adjust. The screws could be replaced by hydraulic push rods to realize electrical control, but the mechanical devices may also affect the performance of the FSS.

IV. CONCLUSION

In this paper, a novel mechanically tunable FSS based on sliding inserted dielectric is proposed. By analyzing the working mechanism of the traditional FSS, we use the sliding 3D-printed inserted dielectric to change the equivalent capacitance of the 3D-FSS slots and then achieve tunability. To optimize the performance, an improved structure based on a hollow support and a tripole slot is proposed. The simulation results show that the improved structure has both a wide tunable range and good angular stability.

To verify this idea, we fabricated a cross slot prototype by 3D printing and mechanical engraving. Measured results show that this prototype has a continuous tunable range of 34.4%. The measurement tolerance has been explained

in detail. Finally, we have discussed the advantages and disadvantages of the proposed tunable FSS. Several suggestions for improvement have also been made. In general, the tunable FSS based on an inserted dielectric appears to provide a good mechanical solution to achieve wide tunability without the use of PCB technology and active components. With the development of 3D printing technology and material science, this tunable FSS may have good potential.

REFERENCES

[1] X. G. Huang, Z. Shen, Q. Y. Feng, and B. Li, "Tunable 3-D bandpass frequency-selective structure with wide tuning range," *IEEE Trans. Antennas Propag.*, vol. 63, no. 7, pp. 3297–3301, Jul. 2015.
[2] A. Ebrahimi, Z. Shen, W. Withayachumnankul, S. F. Al-Sarawi, and D. Abbott, "Varactor-tunable second-order bandpass frequency-selective surface with embedded bias network," *IEEE Trans. Antennas Propag.*, vol. 64, no. 5, pp. 1672–1680, May 2016.
[3] S. Ghosh and K. V. Srivastava, "Broadband polarization-insensitive tunable frequency selective surface for wideband shielding," *IEEE Trans. Electromagn. Compat.*, vol. 60, no. 1, pp. 166–172, Feb. 2018.
[4] Q. Guo, Z. Li, J. Su, J. Song, and L. Y. Yang, "Active frequency selective surface with wide reconfigurable passband," *IEEE Access*, vol. 7, pp. 38348–38355, 2019.
[5] A. E. Martynyuk, J. I. M. Lopez, and N. A. Martynyuk, "Active frequency-selective surfaces based on loaded ring slot resonators," *Electron. Lett.*, vol. 41, no. 1, pp. 2–4, Jan. 2005.
[6] G. I. Kiani, K. L. Ford, L. G. Olsson, K. P. Esselle, and C. J. Panagamuwa, "Switchable frequency selective surface for reconfigurable electromagnetic architecture of buildings," *IEEE Trans. Antennas Propag.*, vol. 58, no. 2, pp. 581–584, Feb. 2010.
[7] D. F. Mamedes, A. Gomes Neto, J. C. E. Silva, and J. Bornemann, "Design of reconfigurable frequency-selective surfaces including the PIN diode threshold region," *IET Microw., Antennas Propag.*, vol. 12, no. 9, pp. 1483–1486, Jul. 2018.
[8] R. Phon, S. Ghosh, and S. Lim, "Novel multifunctional reconfigurable active frequency selective surface," *IEEE Trans. Antennas Propag.*, vol. 67, no. 3, pp. 1709–1718, Mar. 2019.
[9] W. Hu, R. Dickie, R. Cahill, H. Gamble, Y. Ismail, V. Fusco, D. Linton, N. Grant, and S. Rea, "Liquid crystal tunable mm wave frequency selective surface," *IEEE Microw. Wireless Compon. Lett.*, vol. 17, no. 9, pp. 667–669, Sep. 2007.
[10] M. Sazegar, Y. Zheng, C. Kohler, H. Maune, M. Nikfalazar, J. R. Binder, and R. Jakoby, "Beam steering transmitarray using tunable frequency selective surface with integrated ferroelectric varactors," *IEEE Trans. Antennas Propag.*, vol. 60, no. 12, pp. 5690–5699, Dec. 2012.
[11] M. Haghzadeh, C. Armiento, and A. Akyurtlu, "All-printed flexible microwave varactors and phase shifters based on a tunable BST/Polymer," *IEEE Trans. Microw. Theory Techn.*, vol. 65, no. 6, pp. 2030–2042, Jun. 2017.
[12] D. Wang, W. S. Zhao, H. Xie, and J. Hu, "Tunable THz multiband frequency-selective surface based on hybrid metal–graphene structures," *IEEE Trans. Nanotechnol.*, vol. 16, no. 6, pp. 1132–1137, Nov. 2017.
[13] S. N. Azemi, K. Ghorbani, and W. S. T. Rowe, "A reconfigurable FSS using a spring resonator element," *IEEE Antennas Wireless Propag. Lett.*, vol. 12, pp. 781–784, 2013.
[14] B. J. Lei, A. Zamora, T. F. Chun, A. T. Ohta, and W. A. Shiroma, "A wideband, pressure-driven, liquid-tunable frequency selective surface," *IEEE Microw. Wireless Compon. Lett.*, vol. 21, no. 9, pp. 465–467, Sep. 2011.
[15] M. Li and N. Behdad, "Fluidically tunable frequency selective/phase shifting surfaces for high-power microwave applications," *IEEE Trans. Antennas Propag.*, vol. 60, no. 6, pp. 2748–2759, Jun. 2012.
[16] D. Ferreira, I. Cuinas, R. F. S. Caldeirinha, and T. R. Fernandes, "3-D mechanically tunable square slot FSS," *IEEE Trans. Antennas Propag.*, vol. 65, no. 1, pp. 242–250, Jan. 2017.
[17] K. Fuchi, J. Tang, B. Crowgey, A. R. Diaz, E. J. Rothwell, and R. O. Ouedraogo, "Origami tunable frequency selective surfaces," *IEEE Antennas Wireless Propag. Lett.*, vol. 11, pp. 473–475, 2012.
[18] M. Safari, C. Shafai, and L. Shafai, "X-band tunable frequency selective surface using MEMS capacitive loads," *IEEE Trans. Antennas Propag.*, vol. 63, no. 3, pp. 1014–1021, Mar. 2015.
[19] J. M. Zendejas, J. P. Gianvittorio, Y. Rahmat-Samii, and J. W. Judy, "Magnetic MEMS reconfigurable frequency-selective surfaces," *J. Microelectromech. Syst.*, vol. 15, no. 3, pp. 613–623, Jun. 2006.
[20] B. A. Munk, *Frequency Selective Surfaces: Theory and Design*. New York, NY, USA: Wiley, 2000.

SHIHAO QIU (Graduate Student Member, IEEE) received the B.S. degree in electronic information engineering from Xidian University, Xi'an, China, in 2015, the M.S. degree in electromagnetic field and microwave technology from East China Normal University, Shanghai, China, in 2018. He is currently pursuing the Ph.D. degree with the Communication University of China, Beijing, China. His current research interests include frequency selective surface and microwave absorption.

QINGXIN GUO (Senior Member, IEEE) received the B.S., M.S., and Ph.D. degrees from the Communication University of China, Beijing, China, in 1997, 2006, and 2013, respectively, all in electromagnetic field and microwave technology.

From 1997 to 2002, he was an Engineer with Xiamen Overseas Chinese Electronics Company Ltd., where he was involved with the repeaters and the mobile phone for the GSM system. From 2002 to 2004, he was a Project Manager of Beijing Gigamega Electronics Company Ltd., where he was responsible for the design of amplifier for transmitter. From 2004 to 2008, he was an Engineer and a Project Manager of Beijing Filcom Technology Company Ltd., where he was responsible for the design of combiner and multiplexer. In 2006, he joined the Communication University of China. From 2011 to 2012, he was a Visiting Researcher with the Electromagnetic Communication laboratory (EMC Lab), which is affiliated with the Electrical Engineering Department, Pennsylvania State University. Since 2013, he has been an Associate Professor with the School of Information Engineering, Communication University of China. His research interests include the antennas, microwave passive components, RF circuits, and metamaterial.

ZENGRUI LI (Member, IEEE) received the B.S. degree in communication and information system from Beijing Jiaotong University, Beijing, China, in 1984, and the M.S. degree from the Beijing Broadcasting Institute, Beijing, in 1987, and the Ph.D. degree from Beijing Jiaotong University, in 2009, both in electrical engineering. From 2004 to 2005, he has studied with Yokohama National University, Japan.

He is currently a Professor with the Communication University of China, Beijing. His research interests include the areas of finite-difference time-domain (FDTD) methods, electromagnetic scattering, metamaterials, and antennas. He is a Senior Member of the Chinese Institute of Electronics.